2008 International Symposium on Nonlinear Theory and its Applications
NOLTA'08, Budapest, Hungary, September 7-10, 2008

Coexisting Oscillations in MEMS Pulsed Digital Oscillators

Denis Bourke and Orla Feely

School of Electrical, Electronic and Mechanical Engineering,
University College Dublin, Dublin 4, Ireland
Email: denisbourke@gmail.com, orla.feely@ucd.ie

Abstract–This paper analyses the behaviour of a class of MEMS pulsed digital oscillators (PDO) using a non-linear iterative model. Previous work has shown that in these systems the normalised oscillation frequency as a function of normalised natural frequency is similar to the devil's staircase fractal. It has also been shown for the most basic such oscillator that several limit cycles can coexist. This means that the steady state oscillation frequency cannot always be uniquely determined by the system parameters, without knowing the initial conditions as well. This effect is explored in greater detail in this paper, and the investigation is widened to include a broader class of PDO topologies.

1. Introduction

Micro-electro-mechanical (MEMS) resonators have a number of advantages in the delivery of high-quality stable oscillations, and find use in applications such as accelerometers and RF components. The pulsed-digital oscillator (PDO) [1] employs a MEMS resonator in a feedback loop familiar from the domain of sigma-delta (ΣΔ) modulation [2]. The aim of this design is to overcome a number of difficulties in the design of large-signal MEMS oscillators, many of them arising out of the nonlinear actuation of standard schemes.

Like the most basic ΣΔ modulator, the PDO involves one-bit quantization in the feedback loop along with the MEMS resonator, greatly simplifying the design and implementation of these systems. It is not surprising, therefore, that the PDO should exhibit nonlinear behaviour similar to that observed in ΣΔ modulators [3]. In particular, it was observed in [1] that the graph of the normalised oscillation frequency as a function of normalised natural frequency of the resonator contains a series of steps, similar to the Devil's staircase fractal also observed in ΣΔ modulators. Teplinsky and Feely [4] have recently undertaken an analysis of the PDO from [1], applying methods of nonlinear dynamics to explain the appearance of this behaviour. It was also shown in [4] that the steps of the devil's staircase can overlap, which means that multiple oscillations can coexist for the same parameters and the initial conditions will determine which of them will be observed in practice.

This paper contains a fuller exploration of this phenomenon, presenting the extent of overlap of the steps for the basic PDO from [1] and also investigating whether the same effect is observed in the broader class of PDOs studied in [5].

2 Pulsed Digital Oscillators

MEMS resonators normally require linear actuation and position sensing of the mechanical element. To avoid this, in the PDO from [1], shown in Figure 1, the oscillator position is sampled and a comparator detects whether it is above or below its equilibrium position. The comparator output is delayed and fed back to the resonator as a force pulse (of uniform magnitude). We will consider here the case where there is one delay in the feedback loop, though more delays can also be incorporated.

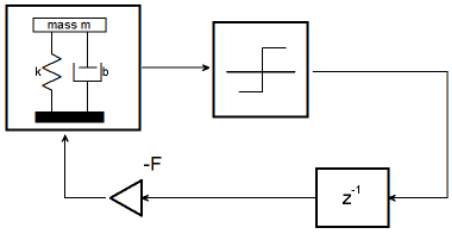

Figure 1. The MEMS oscillator from [1].

The force pulse, ideally a delta function, can take on only two values, +F or –F, so the actuation mechanism need not be linear. The position detection mechanism can also be very basic, since it only needs to detect if the oscillator is above and below the equilibrium position [1].

The position $x(t)$ of the resonator in the oscillator of Figure 1 is given by the equation

$$m\frac{d^2x(t)}{dt^2}+b\frac{dx(t)}{dt}+kx(t)=-F\sum_n \delta(t-t_n)\,\mathrm{sgn}(x(t_{n-1})), \quad (1)$$

where m is the mass of the moveable plate, b is the damping factor, k is the spring factor, F is the impulse affecting the system at sampling instants $t_n = nT_s$, $\delta(t)$ is the Dirac delta function, and $\mathrm{sgn}(x)=\begin{cases}1 \text{ for } x\geq 0\\ -1 \text{ for } x<0\end{cases}$. The resonator is assumed to be underdamped, i.e. $0<b^2<4km$.

We introduce the variable $y = -\frac{\beta}{\sqrt{1-\beta^2}}x - \frac{1}{\omega_0\sqrt{1-\beta^2}}v$, where $\beta = b/\left(2\sqrt{km}\right) \in (0,1)$ is the dimensionless damping factor, $\omega_0 = \sqrt{k/m}$ is the natural frequency of the resonator and $v(t) = \frac{dx(t)}{dt}$. It is shown in [4] that the values $x_n = x(nT_s)$ and $y_n = y(nT_s+)$ at the sampling instants nT_s obey the following 2-dimensional iterative system:

$$\begin{pmatrix} x_{n+1} \\ y_{n+1} \end{pmatrix} = f\begin{pmatrix} x_n \\ y_n \end{pmatrix} \stackrel{\text{def}}{=} a\mathbf{R}(2\pi r)\begin{pmatrix} x_n \\ y_n \end{pmatrix} + \begin{pmatrix} 0 \\ Y \end{pmatrix}\text{sgn}(x_n), \tag{2}$$

where $\mathbf{R}(\alpha) = \begin{pmatrix} \cos\alpha & -\sin\alpha \\ \sin\alpha & \cos\alpha \end{pmatrix}$ is the matrix of the (counter-clockwise) rotation by angle α, $r = T_s\frac{\omega_0}{2\pi}\sqrt{1-\beta^2}$ is the normalized sampling ratio, $a = \exp(-2\pi\frac{\beta}{\sqrt{1-\beta^2}}r) \in (0,1)$ is the contraction factor and $Y = \frac{F}{\omega_0 m\sqrt{1-\beta^2}}$ represents the instantaneous change in velocity due to the force delta.

The oscillations displayed by the MEMS oscillator correspond to stable limit cycles of (2). These limit cycles are stable under small perturbations of r and β, and so if we plot the rotation number ρ, the average steady-state rotation of a trajectory about the origin per sampling period, as a function of r we get a sequence of steps of the familiar devil's staircase from [3]. Increasing the level of damping increases the tendency for frequencies to lock over a larger region, so the steps, particularly those for low-denominator ρ, are wider.

Figure 2 plots the rotation number ρ of (2) as a function of normalized sampling ratio r for two values of β, 0.05 and 0.005. The staircase nature of the relationship is clear, particularly for larger values of β. It is also clear that, unlike the classical devil's staircase, this graph has overlapping steps, corresponding to coexisting limit cycles. This clearly limits the ability of the oscillator to deliver the required oscillation. In this system, this effect is particularly pronounced for large values of β and of r.

Apart from the instantaneous change in velocity with each force pulse the resonator is oscillating freely, so the oscillation frequency is close to the natural oscillation frequency and the rotation number ρ is close to r. It can be seen, even examining only the underlying trend of the graph, that larger values of damping lead to greater divergence of the oscillation frequency from the natural frequency of the resonator.

When multiple oscillations coexist, it is necessary to examine their basins of attraction in order to ascertain which is most likely to be observed in practice. Figure 3 shows the basins of attraction of three limit cycles for β = 0.05 and r = 0.45.

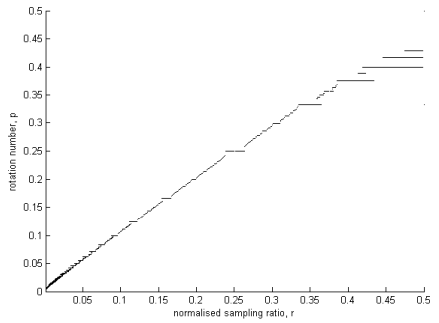

(a)

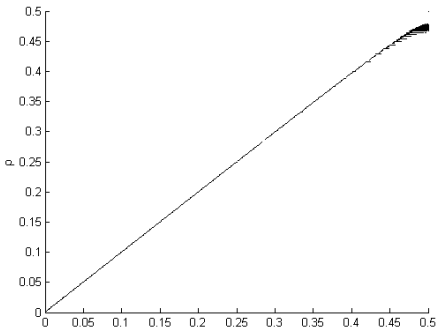

(b)

Figure 2 Rotation number ρ of (2) as a function of normalized sampling ratio r with β = (a) 0.05 (b) 0.005.

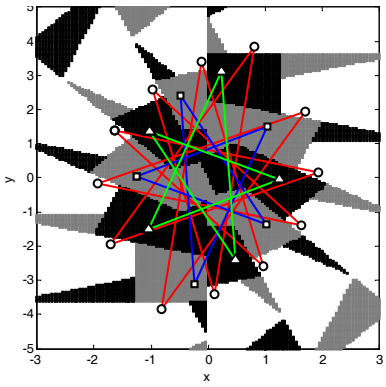

Figure 3 Basins of attraction for the three coexisting limit cycles for β = 0.05 and r = 0.45. The limit cycle with successive points marked joined by red lines is approached by trajectories starting in the white areas, and has ρ = 5/12. Trajectories starting from the grey region approach the limit cycle joined with blue lines and those starting from the black region approach the limit cycle marked in green. The last two both have ρ = 2/5, but the resulting oscillations will have different phases.

3. Double feedback PDO

In [5], Dominguez et al describe a double-feedback PDO topology, which incorporates digital FIR filtering into the feedback loop. The aim of this filtering is to minimise the effects of damping losses mentioned

previously: the divergence of the oscillation frequency from the natural frequency of the resonator and the fractal nature of that response. What was not considered in [5] is the possibility of coexisting oscillations in this new topology, and it is that coexistence that we seek to examine here. Two topologies are investigated (see fig 4) for cases $\gamma = 0$ and $\gamma = 1$.

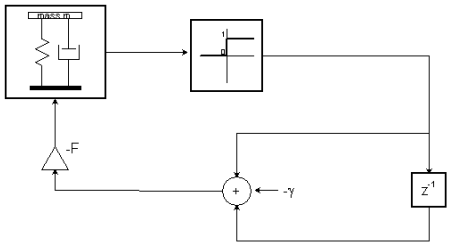

Figure 4 Double-feedback PDO topologies. γ =e 0 or 1, Note the comparator outputs zero or one here.

For both cases, the underlying trend of the graph is closer to the identity line than it is in the 1-delay topology. This is countered however by a greater overlap of the steps for low *r*, as shown in Figures 5 and 6. The basins of attraction of the low-denominator cycles can be small, as shown in Figure 7, but they do exist, and the system can deliver an unwanted oscillation of this kind.

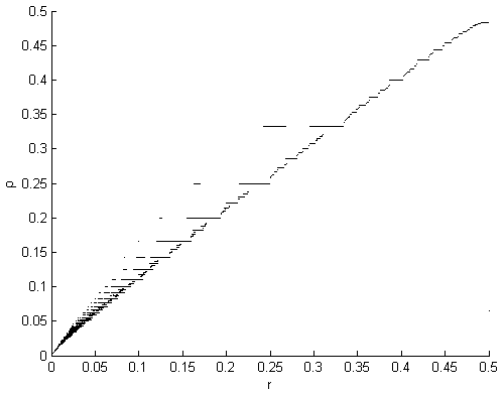

(a)

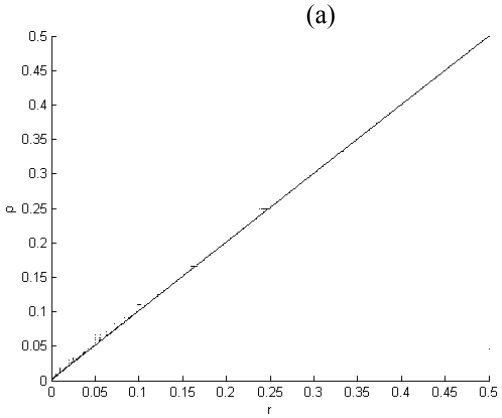

(b)

Figure 5 Rotation number ρ of the system of Figure 4 with $\gamma = 0$ as a function of normalized sampling ratio *r* with β = (a) 0.05 (b) 0.005.

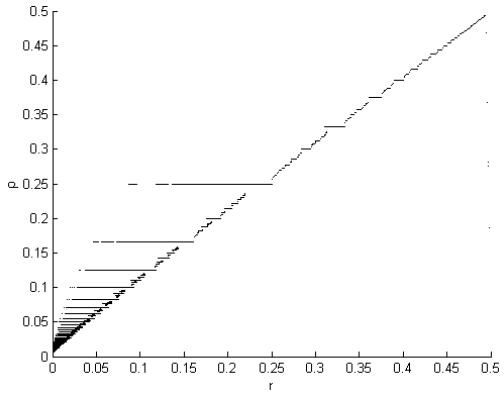

(a)

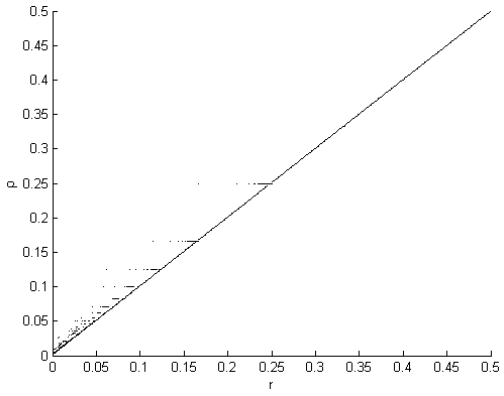

(b)

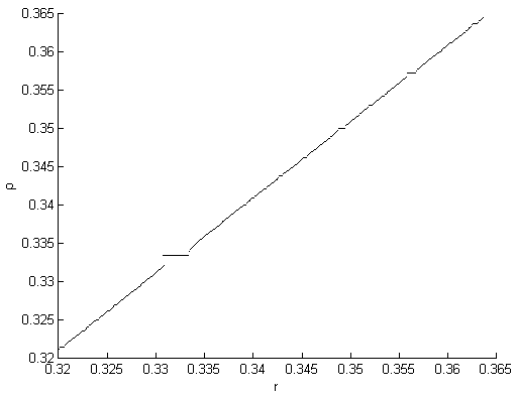

(c)

Figure 6 Rotation number ρ of the system of Figure 4 with γ = 1 as a function of normalized sampling ratio *r* with β = 0.05 (a) 0.005 (b) and a close-up of the plot with β=0.005 (c).

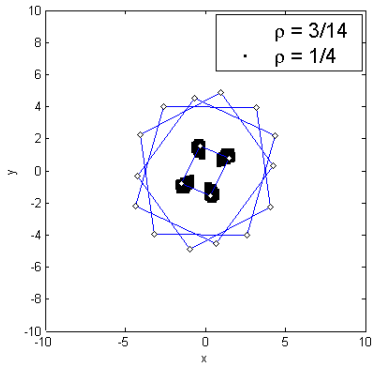

Figure 7 Basins of attraction of the system of Figure 4 with γ = 1, with $\beta = 0.005$ and $r = 0.2$. The white area is the basin of attraction of a limit cycle with $\rho = 3/14$, and the black area is the basin of attraction of a limit cycle with $\rho = 1.4$.

There are, of course, many other possible topologies. A further double-feedback topology is shown in Figure 8, where a second delay is introduced into the feedback path.

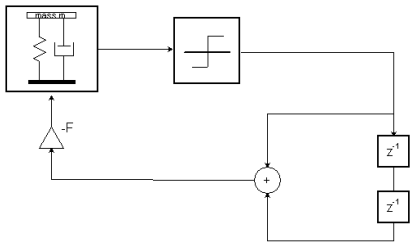

Figure 8; Double feedback topology with two delays.

For this topology, for smaller values of r, the relationship between ρ and r is very close to linear, but it diverges significantly for larger values, as illustrated in figure 9.

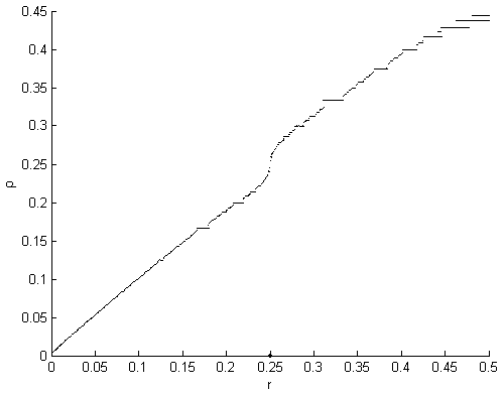

Figure 9; Topology with two delays for β=0.05.

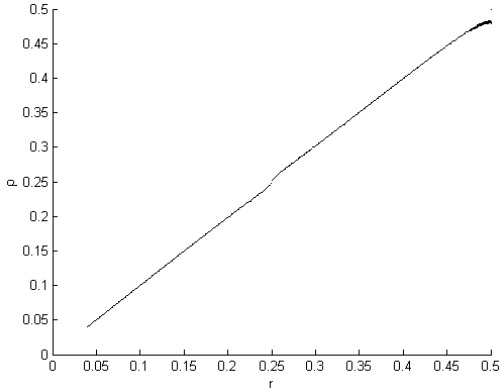

Figure 10; Topology with two delays for β=0.005.

4. Conclusion

Several PDO topologies have been examined here, with particular reference to the divergence of their oscillation frequency from their natural frequency, as well as the possibility of coexisting oscillations. These aspects of the behaviour depend in particular on the level of damping and on the normalised natural frequency of the resonator.

The influence of initial conditions on the oscillator frequency depends greatly on the feedback topology used. The oscillation frequency can also be brought closer to the natural resonator frequency by appropriate choice of feedback topology. This choice will also depend on the levels of damping encountered and on the range of frequency output required. For applications where a broad range of frequency outputs is required, appropriate feedback can be switched in.

References

[1] M. Dominguez, J. Pons-Nin, J. Ricart, A. Bermejo, E. F. Costa, and M. Morata, "Analysis of the Σ-Δ pulsed digital oscillator for MEMS," *Circuits and Systems I: Regular Papers, Fundamental Theory and Applications, IEEE Transactions on,* vol. 52, pp. 2286-2297, 2005.

[2] R. Schreier and G. C. Temes, *Understanding Delta-Sigma Data Converters*: Wiley-IEEE Press, 2004.

[3] O. Feely, "A tutorial introduction to nonlinear dynamics and chaos and their application to sigma-delta modulators," *Int. J. Circuit Theory and Applications*, vol. 25, pp. 347-367, Sept. 1997.

[4] A. Teplinsky and O. Feely, "Limit cycles in a MEMS Oscillator," *IEEE Transactions on Circuits and Systems II: Express Briefs,* to appear, 2008.

[5] M. Dominguez, J. Pons, J. Ricart, J. Juillard, and E. Colinet, "Linear analysis of the influence of FIR feedback filters on the response of the pulsed digital oscillator," *Analog Integr Circ Sig Process,* vol. 53, pp. 145-152, 2007.